

Journal Pre-proofs

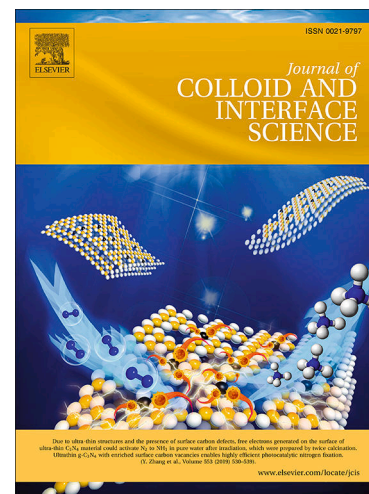
Shear-induced nanostructural changes in micelles formed by sugar-based surfactants with varied anomeric configuration

Johan Larsson, Ashley P. Williams, Marie Wahlgren, Lionel Porcar, Stefan Ulvenlund, Tommy Nylander, Rico F. Tabor, Adrian Sanchez-Fernandez

PII: S0021-9797(21)01237-6
DOI: <https://doi.org/10.1016/j.jcis.2021.08.007>
Reference: YJCIS 28536

To appear in: *Journal of Colloid and Interface Science*

Received Date: 26 June 2021
Revised Date: 13 July 2021
Accepted Date: 1 August 2021



Please cite this article as: J. Larsson, A.P. Williams, M. Wahlgren, L. Porcar, S. Ulvenlund, T. Nylander, R.F. Tabor, A. Sanchez-Fernandez, Shear-induced nanostructural changes in micelles formed by sugar-based surfactants with varied anomeric configuration, *Journal of Colloid and Interface Science* (2021), doi: <https://doi.org/10.1016/j.jcis.2021.08.007>

This is a PDF file of an article that has undergone enhancements after acceptance, such as the addition of a cover page and metadata, and formatting for readability, but it is not yet the definitive version of record. This version will undergo additional copyediting, typesetting and review before it is published in its final form, but we are providing this version to give early visibility of the article. Please note that, during the production process, errors may be discovered which could affect the content, and all legal disclaimers that apply to the journal pertain.

Shear-induced nanostructural changes in micelles formed by sugar-based surfactants with varied anomeric configuration

Johan Larsson,^{a,1} Ashley P. Williams,^b Marie Wahlgren,^{c,d} Lionel Porcar,^e Stefan Ulvenlund,^{c,d} Tommy Nylander,^{a,f} Rico F. Tabor,^b Adrian Sanchez-Fernandez.^{c,*}

Johan Larsson: Methodology, Investigation, Formal analysis, Writing - original draft. **Ashley P. Williams:** Investigation, Software, Formal analysis, Writing - review & editing. **Marie Wahlgren:** Methodology, Writing - review & editing. **Lionel Porcar:** Investigation, Resources, Writing - review & editing. **Stefan Ulvenlund:** Methodology, Writing - review & editing, Funding acquisition. **Tommy Nylander:** Methodology, Writing - review & editing, Funding acquisition. **Rico F. Tabor:** Methodology, Software, Writing - review & editing. **Adrian Sanchez-Fernandez:** Conceptualization, Methodology, Formal analysis, Writing - review & editing.

^aPhysical Chemistry, Department Chemistry, Lund University, Box 124, 221 00 Lund, Sweden.

^bSchool of Chemistry, Monash University, Clayton, VIC 3800, Australia

^cFood Technology, Nutrition and Engineering, Lund University, Box 124, 221 00 Lund, Sweden.

^dEnza Biotech AB, Scheelevägen 22, 22363 Lund, Sweden.

^eInstitut Laue-Langevin, DS / LSS, 71 avenue des Martyrs, 38000, Grenoble, France.

^fNanoLund, Lund University, Lund, Sweden

*Corresponding author: adrian.sanchez-fernandez@food.lth.se

¹Present address: Department of Biomedical Science and Biofilms—Research Center for Biointerfaces, Malmö University, Jan Waldenströms gata 25, 214 28 Malmö, Sweden.

Hypothesis: The self-assembly of long tail sugar-based surfactants into worm-like micelles has recently been demonstrated, and the rheological properties of such systems have been shown to be tuneable through subtle modifications of the molecular characteristics of the surfactant monomer. In particular, the anomeric configuration of the hexadecylmaltoside headgroup was shown to induce profound changes in the nanostructure and rheology of the system. The origin of such changes is hypothesised to arise from differences in the structure and relaxation of the micellar networks in the semi-dilute regime.

Experiments: Here we explore the molecular background to the flow properties of the two anomers of hexadecylmaltoside (α - and β -C₁₆G₂) by directly connecting their rheological behaviour to the micelle morphology. For this purpose, 1-3 plane rheo-small-angle neutron scattering measurements, using a Couette cell geometry, probed the structural changes in the micellar phase under shear. The effect of surfactant anomeric configuration, surfactant concentration, temperature and mixing ratio of the two anomers were investigated. The static micelle structure in the semi-dilute regime was determined using the polymer reference interaction site model.

Findings: The segmental alignment of the micellar phase was studied under several flow conditions, showing that the shear-thinning behaviour relates to the re-arrangement of β -C₁₆G₂ worm-like micelles, whilst shorter α -C₁₆G₂ micelles are considerably less affected by the flow. The results are rationalised in terms of micelle alignment and disruption of the entangled network, providing a detailed mechanism by which sugar-based surfactants control the rheology of the fluid. To further enable future studies, we provide the complete code for modelling micelle structure in the semi-dilute regime using the polymer reference interaction site model.

Introduction

As society moves towards more environmentally friendly technologies, there is a need for sustainable surfactants that can give functional properties to consumer products (e.g. cosmetics and pharmaceutical formulations). Several of the relevant surfactants currently used in formulation technology are produced using chemicals derived from fossil raw materials (e.g. polysorbates and other ethoxylated systems). In addition, some ionic surfactants should be avoided in formulation technology as they can be harmful for the body (e.g. cause irritation in the skin or mucosa). Sugar-based surfactants, such as the maltoside surfactants used in this study, have low toxicity and can be produced using renewable

materials and ‘green’ synthesis pathways [1]. The introduction of sugar-based surfactants is therefore part of the transition toward more environmentally friendly products that is currently taking place.

Self-assembled surfactant structures can be used to promote specific rheological properties in the system, such as shear-thinning behaviour and viscoelasticity. This is highly relevant in myriad formulated products, such as shampoos, shower gels, cosmetic creams, or pharmaceutical dispersions [2], as it confers the required characteristics for handling, administration, and stabilisation to the systems. Specifically, surfactants that form worm-like micelles (WLM) in solution bestow these properties. WLM are semiflexible elongated self-assembled structures, sometimes referred to as “living polymers” [3]. In solution, above the overlap concentration, they entangle, resulting in intriguing and useful rheological behaviour [4]. At rest or low shear stress, WLM entanglement results in an increase in viscosity. With increasing shear stress the network rearranges through different relaxation modes and the viscosity of the system gradually decreases [3]. Thus, WLM solutions behave as non-Newtonian shear-thinning fluids. The entanglements also gives WLM solutions viscoelastic properties, meaning that at short time scales they behave as an elastic material and at long time scales they behave as a viscous material [5]. Polymers in solution behave in a similar way but, unlike polymers, WLM subunits (i.e. surfactant monomers) are not covalently bound. Thus, WLM are equilibrium structures, which continuously break and reform, giving rise to different relaxation modes (e.g. reptation and breakage). Nevertheless, these systems can generally be described by a single relaxation time (τ), which is obtained from the frequency at which the viscous and elastic moduli have identical values [6].

As the change in the rheological behaviour from that of a dilute WLM dispersion is attributed to the formation of an entangled network, the shear thinning has been related to the disruption of such a network when stress is applied [7]. A common picture is to attribute the change in viscosity to the alignment of the WLM in the flow direction [8, 9]. In addition, other relaxation modes can be observed in WLM systems under shear. Simulations have shown that micelle rupture increases with shear, resulting in a decrease of the mean micelle length, which becomes a contributing factor to the shear thinning behaviour [10].

Since flow properties are singularly relevant for several of the applications of WLM (e.g. drag-reducing agents and rheology modifiers), it is important to understand the effect of flow on the WLM systems. Rheo-SANS is a technique which combines rheometry and small-angle neutron scattering (SANS) to study the structure of colloidal systems when subjected to shear [11, 12]. With rheo-SANS, a sample can be examined in three different planes upon shearing (flow-vorticity (1-3), gradient-vorticity (2-3) and flow-gradient (1-2)) by varying the angle and position of the sample relative to the incident beam, yielding complementary information [11]. Measurements in the 1-3 plane provide information on the average structure across the gap of the Couette and can be used to detect inhomogeneities along the vertical vorticity direction. The 2-3 plane is investigated by aligning the neutron beam tangentially to the sheared sample. When studying the 1-2 plane the cell is rotated 90° to have to axis of rotation parallel to the beam.

Rheo-SANS has been used in several studies of WLM and has been able to give a deeper understanding of the microscopic origin of their rheological behaviour. Measurements in the 1-3 plane were used to show that WLM align in the flow direction [13, 14], that the alignment increases with increasing shear rate and that there is an exponential dependence between the alignment and the viscosity [15]. Measurements along the 1-2 plane of a WLM system formed by a cationic/anionic surfactant mixture of 1.5 wt% CTAT and SDBS in D₂O showed that the alignment is increasing with decreasing distance to the moving cylinder wall and that the onset of the shear thinning regime coincide with the onset of alignment closest to the moving wall [16]. Scattering from the 1-2 plane also revealed that several WLM systems separate into two phases during shear, one isotropic low shear phase close to the static wall and one anisotropic high shear phase close to the moving cylinder, a phenomenon referred to as shear banding [8, 17, 18]. There are also WLM systems where no shear banding arises and this was attributed to the formation of branched micelles [19]. Almost all surfactant systems investigated by rheo-SANS have been based on ionic surfactants, but there are a few studies of non-ionic surfactants showing alignment of elongated micelles [20, 21]. Similar to the ionic systems, non-ionic elongated micelles were observed to align with flow and this, in turn, was shown to be connected to the rheology of the system. As such, C₁₆E₆, was shown to form relatively short rod-like micelles that aligned at very high shear rates [20]. On the contrary, a novel class of sugar-based surfactants with a polyethylene glycol linker forms WLM that showed an onset of alignment at much lower shear rates, *ca.* 10 s⁻¹ [21]. With this background, we begin to grasp the mechanistic origin of the shear thinning behaviour of WLM systems. However, further investigations are required to elucidate the

connection between the nanostructure of the micellar phase and the macroscopic response of the system under flow, especially those composed by non-ionic micelles.

The self-assembly and rheological behaviour of the two anomers of hexadecylmaltoside (α - and β -C₁₆G₂) have been previously investigated [22, 23]. It was shown that these surfactants form elongated micelles in solution, which results in interesting rheological properties that can be modulated by blending the two anomers. It was also shown that the elongation can be controlled with variation of both concentration and temperature. This possibility to control the micelle morphology, from globular micelles to WLM, allows for fine tuning of the rheological properties of the system. In the present work, we use rheo-SANS to investigate the α - and β -C₁₆G₂ systems in order to determine the mechanistic origin of their shear thinning behaviour. Here, the effect of shear upon the nanostructure of the system is reported under different conditions (temperature, surfactant concentration, and mixing ratio) and connected to the rheological behaviour of the system.

Experimental

Materials

n-Hexadecyl- α -D-maltopyranoside (α -C₁₆G₂) was purchased from Ramidus AB and n-hexadecyl- β -D-maltopyranoside (β -C₁₆G₂) was purchased from Anatrace Inc. The purity of these surfactants is $\geq 97\%$, as confirmed by HPLC chromatography [22]. D₂O was purchased from Sigma Aldrich (99.9% atom-D). Surfactant solutions in D₂O were prepared under mild agitation at 40 °C.

Static SANS

Small-angle neutron scattering from the surfactant systems in the absence of shear was measured to determine the structure of the micelles. SANS data were acquired on D22 at the Institute Laue-Langevin (Grenoble, France). Samples were loaded in 2 mm cylindrical quartz Hellma cells and placed in a temperature-controlled sample changer at 50 °C for measurement. The front detector was placed at 1.3 m, and the rear detector was placed at 5.6 m and 17.6 m from the sample position, and a rectangular sample aperture of 7×10 mm was used. Two neutron wavelengths were used for these measurements, 6 Å and 11.5 Å. These configurations provided a combined q-range of 0.00151–0.59 Å⁻¹. The raw data was reduced according to the D22 protocols using the GRASP software [24].

Analysis of the micelle structure was performed using a model-based approach. As the micelle volume fractions investigated here are in the semi-dilute regime, intermicellar interactions needed to be accounted for. The polymer reference interaction site model (PRISM) was used to determine the direct correlation function, $\beta c(q)$, which accounts for intermicellar correlations between elongated micelles. The combination of the PRISM model with the flexible cylinder form factor thus determines the scattering for WLM with intra- and intermicellar excluded volume effects. It should be noted that this model was validated using closed-form Monte Carlo simulations of interacting WLM. Some of the parameters used in the model are empirical in nature and their relationship to physical aspects of the system is yet to be unambiguously isolated [25, 26]. This model has also successfully been used to analyse SANS data from WLM in the semi-dilute regime [27, 28]. The MATLAB code used for modelling the scattering from WLM in the semi-dilute regime is presented in the Supplementary information. This code is a re-work of the model previously published by Williams *et al.* that expands the applicability of this model to WLM of arbitrary contour length and flexibility [28].

The flexible cylinder-PRISM model uses the following structural parameters to calculate the WLM form factor: the radius of the micelle cross-section (r), the micelle contour length (L), the micelle persistence length (l_p). The structure factor for WLM micelles in the semi-dilute regime is calculated using an effective radius (r_{eff}), the interaction scale factor (B) and the parameter σ . The parameter B relates to the number of special correlations between scatterers due to intermicellar interactions and, as such, describes how much the intermicellar contribution affects the overall scattering. Due to the semi-empirical nature of PRISM, it should be noted that the physical meaning of the parameter σ is yet unknown [25, 26]. Also, the parametrisation of the model gives a strong correlation between r_{eff} and σ . As such, they cannot simultaneously be determined through the analysis of the scattering data. Therefore, the parameter σ was fixed to 1 and held constant during fitting, and r_{eff} was fitted, as this approach has previously been shown to accurately determine the scattering from interacting chains [28]. Note that the physical meaning of the parameter σ is

yet unknown. In addition, the model accounts for the micelle volume fraction, ϕ_m , and the contrast factor, ΔSLD ($\Delta\text{SLD} = \text{SLD}_s - \text{SLD}_m$, where SLD_s is the scattering length density of the solvent and SLD_m is the scattering length density of the micelle). The SLD of the micelle was calculated as that of the surfactant tail as headgroup solvation significantly reduces the contribution from the headgroup region [22]. Thus, the SLD of the micelle was assumed to be uniform, neglecting possible solvation effects, which simplifies the analysis of = scattering data. The scattering length densities were held constant during fitting to the calculated values: $\text{SLD}_s = 6.37 \cdot 10^{-6} \text{ \AA}^{-2}$ and $\text{SLD}_m = -0.40 \cdot 10^{-6} \text{ \AA}^{-2}$ [22]. A polydispersity function was included to account for variations in the size of the micelle cross-section. The size distribution is calculated using a Schulz function parametrised with a polydispersity value of 0.15 [29]. For further information about the parametrisation of the flexible cylinder-PRISM model and about the calculation of the scattering length densities, please refer to our previous publications [22, 28].

Rheo-SANS

The scattering experiment was conducted on D22 at the Institute Laue-Langevin (Grenoble, France). An Anton Paar MCR 501 rheometer with a custom SANS set up was used with a Couette geometry (Searle cell, cup diameter 30 mm; cylinder diameter 28 mm, path length 2 mm) as the sample stage. The temperature in the instrument was set to either 30 or 50 °C for the experiments performed here. The neutron wavelength was 6 Å and three sample-to-detector distances were used (2.8, 5.6 and 17.6 m) which gives access to a sufficiently wide q -range of $0.002581 - 0.3564 \text{ \AA}^{-1}$. These measurements were taken using a circular aperture with a diameter of 7 mm. The data was reduced using the standard protocols of the beamline, accounting for signal of the sample environment, detector efficiency and background noise using the GRASP software [24]. Data is available at doi:10.5291/ILL-DATA.9-10-1610 [30].

Data analysis of isotropic and anisotropic scattering data was done in GRASP. Anisotropic scattering was analysed by averaging the scattered intensity from perpendicular angular sectors (vertical or horizontal) with a fixed angle of 18° (Figure 1). The intensity was also studied as a function of azimuthal angle (φ) in a narrow q -range $q^* = 0.05 \pm 0.005 \text{ \AA}^{-1}$. The zero angle was set in the top section of the detector, as marked in Figure 1b, and increases clockwise around the detector. An alignment factor (A_f) was calculated from the angular intensity according to Equation 1 [16].

$$A_f(q^*) = \frac{\int_0^{2\pi} I(q^*, \varphi) \cos(2(\varphi - \varphi_0)) d\varphi}{\int_0^{2\pi} I(q^*, \varphi) d\varphi} \quad (1)$$

where φ_0 is the angle of maximum intensity, which was defined as the angle zero for the integration. The alignment factor is 0 for an isotropic sample and increases up to a maximum value of 1 with increasing nanoscale alignment.

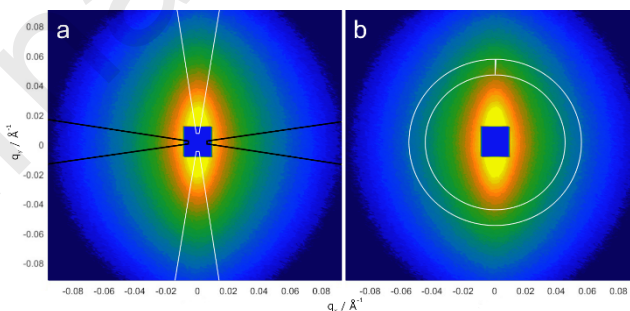


Figure 1. Analysis of anisotropic scattering. (a) vertical (white) and horizontal (black) sectors with an angle of 18° used for averaging anisotropic scattering. (b) section used for the study of intensity as a function of azimuthal angle.

The acquisition times in the SANS experiments were varied for each sample to accumulate at least 2.5×10^6 detector counts per sample, which gives good statistics to our data.

Results

Previous rheological investigations of α - and β - C_{16}G_2 have shown that the behaviour of the system varies with concentration, temperature, and α/β ratio [22, 23]. An overview of the rheology is presented in Figure 2a-c [23]. The two anomers show remarkable differences as β - C_{16}G_2 solutions are highly viscous and non-Newtonian, while α - C_{16}G_2 show low viscosity and a Newtonian behaviour. It was also found that differences in viscosity induced by changes in

temperature and composition mainly appeared at low shear rates. At high shear rates, the differences vanish, and most of the samples show the same viscosity and shear-dependence. Changes in concentration, on the other hand, were found to impact the viscosity over the whole shear rate regime investigated. The difference in the rheological behaviour between the two anomers has previously been attributed to the formation of micelles of different structure. However, the systems were only investigated in the dilute regime and the structure of the micelles in the semi-dilute regime was not determined. In order to reveal the mechanism behind the observed behaviour, static SANS and rheo-SANS experiments were performed on the systems in the semi-dilute regime. The static SANS measurements were focused on the morphological characterisation of the system. The rheo-SANS experiment, where the viscosity was simultaneously monitored as the SANS data were collected, aimed to determine the relation between the structure and rheology of the system. The shear conditions at which the rheo-SANS measurements were performed are presented in Figure 2d.

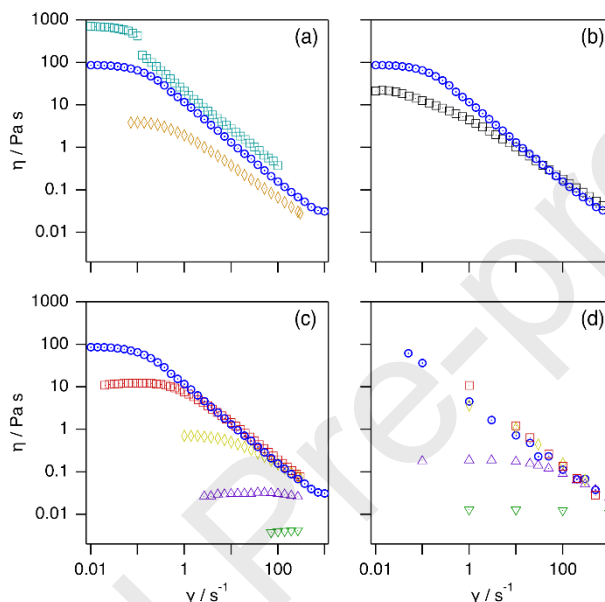


Figure 2. Viscosity versus shear rate for the $C_{16}G_2$ system at different conditions. (a) β - $C_{16}G_2$ at 50 °C at different concentrations in H_2O . 200 (□), 100 (○) and 50 mM (◇). (b) 100 mM β - $C_{16}G_2$ at 50 (○) and 30 °C (□). 100 mM mixtures of α - and β - $C_{16}G_2$ at 50 °C in H_2O (c) and D_2O (d). 100% β (○), 75% β (□), 50% β (◇), 25% β (Δ) and 0% β (▽). (d) Discrete values of the flow curve at which the rheo-SANS measurements were taken. Data included in plots (a), (b), and (c) were reproduced from Larsson *et al.*, Molecular structure of maltoside surfactants controls micelle formation and rheological behavior, *J. Colloid Interface Sci.* 581(Pt B) (2021) 895-904 [23].

The measurements performed using the rheo-SANS setup are in good agreement with the reported behaviour for those surfactants in H_2O [23], i.e. the rheological behaviour evolves from a Newtonian fluid at 100% α - $C_{16}G_2$ to a shear-thinning fluid at 100% β - $C_{16}G_2$. The surfactant mixtures show intermediate values to those of the pure anomers at low shear, whilst they overlap at high shear ($>50 \text{ s}^{-1}$) [23]. Some differences in the absolute values of viscosity can be found between the two configurations. This could be attributed to the influence of the isotopic effect from exchanging H_2O for D_2O , as it has been shown to affect micelle structure and result in larger micelles in D_2O [22, 31, 32].

It is important to note that for the rheo-SANS measurements each point is measured for at least 15 minutes while for the rheology flow curves this was done for 15 seconds. Thus, the rheo-SANS measurements were particularly useful to reveal any time-dependant behaviour. For most of the samples studied no time dependence was observed except for 200 mM β - $C_{16}G_2$, which shows thixotropic behaviour at lower shear rates with a change in viscosity from 1088 to 505 Pas over 30 minutes at a shear rate of 0.05 s^{-1} . This change in the rheological behaviour is observed at the same region where a discontinuity in the flow curve occurs (see Figure 2a) and thus likely has the same root cause.

In the rheo-SANS measurements, the main concentration investigated was 100 mM of surfactant (5.6 wt%). The 2D images of the scattered intensity for the two surfactants under different shear conditions are shown in Figure 3. For 100% β - $C_{16}G_2$ the scattered neutrons transition from an isotropic scattering pattern at low shear rates to a distinct

anisotropic pattern at high shear rates. In contrast, no anisotropic scattering is seen for 100 mM α -C₁₆G₂ up to shear rates of 1000 s⁻¹. This confirms that the stark differences in the rheological behaviour between the two anomers relate to changes in the nanostructure of the system when shear is applied.

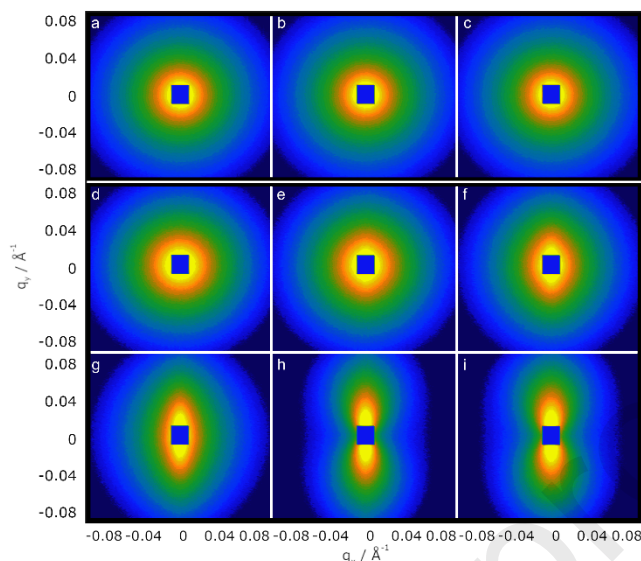


Figure 3. 2D detector images for the 5.6 m sample-to-detector configuration for 100 mM solutions of α -C₁₆G₂ and β -C₁₆G₂ at 50 °C at different shear rates: α -C₁₆G₂ – (a) 0, (b) 100 and (c) 1000 s⁻¹; and β -C₁₆G₂ – (d) 0, (e) 10, (f) 30, (g) 100, (h) 200 and (i) 1000 s⁻¹. High intensity is shown in yellow and low intensity in blue. The blue rectangle in the middle is the beam stop.

Since the difference in the rheological response of the system can be attributed to the formation of different micelle morphologies [12, 23], the micelle structure was investigated under no shear for different concentrations of α -C₁₆G₂ and β -C₁₆G₂. SANS data and best fits using the flexible cylinder-PRISM model are presented in Figure 4, together with the results from the data analysis.

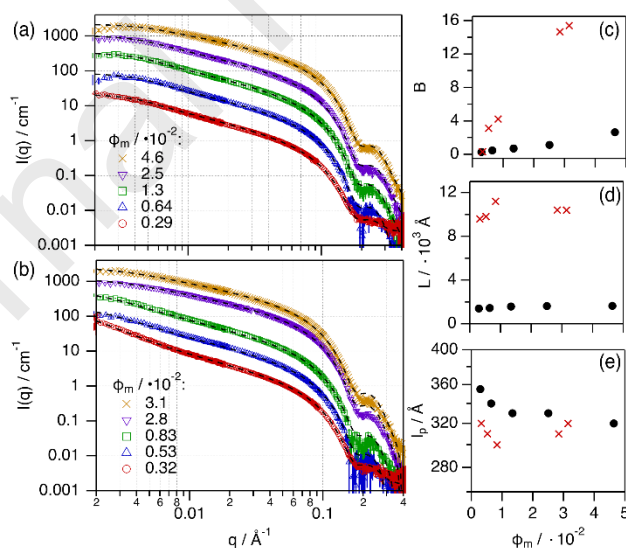


Figure 4. SANS data and best fits of different volume fractions (ϕ_m) of (a) α -C₁₆G₂ and (b) β -C₁₆G₂ at 50 °C under zero shear. The micelle volume fractions are presented in the legend of each graph. The main results from the data analysis are presented as a function of surfactant volume fraction for (●) α -C₁₆G₂ and (×) β -C₁₆G₂: (c) interaction parameter, B, (d) contour length, L, and (e) Kuhn length, l_p . Data and models were scaled for clarity ($\cdot 1$, $\cdot 2$, $\cdot 4$, $\cdot 8$, and $\cdot 16$). Where not visible, error bars are within the marker size.

The surfactant concentrations investigated here cover a range of concentrations from the dilute regime (10 mM, $\phi_m \cong 0.3 \cdot 10^{-2}$) to the semi-dilute regime (up to 200 mM, $\phi_m \cong 4.6 \cdot 10^{-2}$), where the contribution from intermicellar interactions significantly contributes to the scattering curve [22, 23]. From the analysis using the flexible cylinder-

PRISM model, structural and interaction parameters were extracted. It should be noted that there is a certain degree of correlation between the two parameters B and L [28]. To minimise ambiguity in the fitting approach, the results from the analysis of the dilute regime data were used as initial guesses during analysis. The micellar cross-sectional radius is slightly smaller for the α -C₁₆G₂ micelles (21.8 ± 0.4 Å) than for the β -C₁₆G₂ micelles (23.4 ± 0.3 Å), previously attributed to the more extended configuration of the β -C₁₆G₂ headgroup at the micelle interface [22]. When the surfactant concentration is changed in the range investigated here, these values remain unchanged within error. Similarly, the persistence length of the micelles is similar for the two anomers, with an average l_p of 335 ± 20 Å and 315 ± 15 Å for α -C₁₆G₂ and β -C₁₆G₂, respectively, and no major changes are observed with varying the concentration of surfactant. However, the contour length of the micelles differs by a factor of 7, with the β -C₁₆G₂ micelles being longer than the α -C₁₆G₂ ones. These results are consistent with previous investigations that reported that β -C₁₆G₂ forms WLM in the dilute regime, whilst α -C₁₆G₂ assembles into significantly shorter micelles. The effective radius was found to be similar to the radius of the micelle cross-section (27.0 ± 4.0 Å and 27.4 ± 3.8 Å for α -C₁₆G₂ and β -C₁₆G₂, respectively). This value is poorly defined at low micelle volume fractions due to the weak interaction component in the system. A significant difference between the two surfactants is observed in the interaction scale factor B . It is seen that this parameter increases with concentration for both surfactants, but the values are significantly larger in the case of β -C₁₆G₂ in the whole concentration range. This value accounts for the strength of the interaction between micelles and, thus, a higher value relates to stronger interactions. Therefore, the intermicellar interactions in the β -C₁₆G₂ system are more pronounced than in the case of the α -C₁₆G₂ micelles. This is potentially associated with the micelle structure in the semi-dilute regime. The β -C₁₆G₂ system forms longer micelles and thereby there exist more interaction/entanglement points along the micelle contour length, thus increasing the interactions through excluded volume effects.

The rotational diffusion has been shown to decrease with increasing micelle length, resulting in slower relaxations for more elongated structures and the concomitant higher viscosities [33]. Considering the structure of the surfactant micelles and the observed rheological behaviour, the self-assembly of the surfactants directly relates to the macroscopic response of each of the systems investigated here. To further investigate the function-morphology relationship of the micelles under flow, rheo-SANS experiments were conducted. As observed in Figure 3, the anisotropy of the scattered intensity in the 2D detector increases with increasing shear for β -C₁₆G₂. On the other hand, a visual inspection of the data for α -C₁₆G₂ shows no anisotropy in the scattering in the conditions probed here. From these data, the scattering signal in the vertical and horizontal projection of the detector image were calculated as a function of Q . In Figure 5 the scattering in the vertical and horizontal sectors of the 2D data is displayed for 100 mM β -C₁₆G₂ at 50 °C under different shear rates.

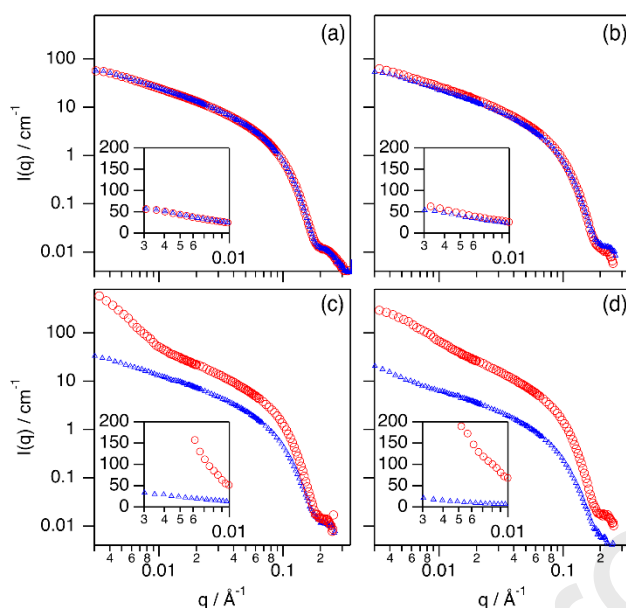


Figure 5. Average intensity from the vertical (Δ) and horizontal (\circ) sectors for 100 mM β -C₁₆G₂ at 50 °C. Results shown for shear rates of 0 (a), 10 (b), 100 (c) and 1000 (d) s⁻¹.

Whilst a perfect overlap is observed for the vertical and horizontal projections of the scattered intensity under no-shear conditions, the scattering at 10 s⁻¹ of shear begins to show a certain degree of anisotropy. The difference between the scattering in the vertical and horizontal projections is more apparent at low Q . At 100 s⁻¹ there is an upturn in the intensity in the vertical sector at ≈ 0.01 Å⁻¹, which is not seen for the horizontal projection. Also, a clear difference in the absolute scattered intensities is observed between the two projections and these differences become more obvious at 1000 s⁻¹. The reason for the upturn around ≈ 0.01 Å⁻¹ is still not clear but suggest the appearance of large structural correlations (>1000 Å) induced by the shear. Such structures have been seen in other WLM systems, for example for hexadecyltrimethylammonium tosylate [34].

In order to probe the source for the difference in the scattering between the two projections, further analysis of the rheo-SANS data was performed. The intensity as a function of azimuthal angle (ϕ) at $q=0.05\pm0.005$ Å⁻¹ for 100 mM β -C₁₆G₂ and α -C₁₆G₂ at 50 °C and different shear rates is shown in Figure 6a and b.

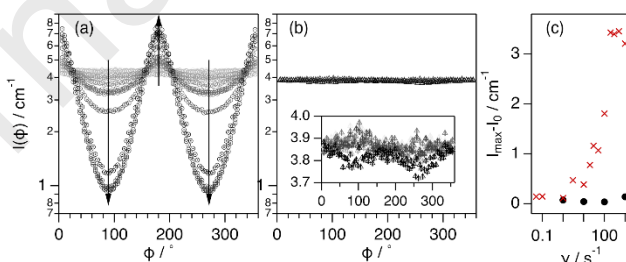


Figure 6. Intensity as a function of azimuthal angle for 100 mM β -C₁₆G₂ at 50 °C (a) and 100 mM α -C₁₆G₂ at 50 °C (b) for $q=0.05\pm0.005$ Å⁻¹ and shear rates from 0 to 1000 s⁻¹. The evolution of the data upon increasing shear follows the direction marked with the black arrows. c) Difference in intensity for different shear rates and at no shear at 180°: β (\bullet) and α (\times).

A visual inspection of the data reveals that there are major differences in the evolution of the scattering upon shear for the two surfactants. The β -C₁₆G₂ solution evolves from an isotropic signal at low shear to a strongly anisotropic signal with two minima at 90° and 270° and two maxima at 180° and 0°/360°. In stark contrast, the signal from the α -C₁₆G₂ solution remains flat except for the highest shear rate, 1000 s⁻¹, where very subtle oscillations are observed. When plotting the difference between the maximum scattered intensity and the zero-shear scattered intensity for each shear rate against the shear rate, it is observed that the evolution of the signal is also different for each surfactant. For β -C₁₆G₂ an increase in the intensity is observed beyond 1 s⁻¹ shear rate. Above that shear rate, the intensity difference gradually increases when increasing shear rate up to around 300 s⁻¹. Above 300 s⁻¹, a plateau at high intensity is reached.

At the highest shear rate, 1000 s^{-1} a minor drop in the intensity is observed. This drop in maximum intensity at high shear rates has been seen for another sugar-based surfactant system where it was explained as slip at the wall of the geometry and, thus, it should not carry major structural implications [21]. For $\alpha\text{-C}_{16}\text{G}_2$ the variation in intensity at different shear rates becomes rather small. However, a small increase in the intensity is observed at the highest shear rate, 1000 s^{-1} . As the differences in the scattered intensity are so small (see Figure 6c), these could be attributed to subtle segmental alignment of the $\alpha\text{-C}_{16}\text{G}_2$ short rods at highest shear rates.

In order to relate the scattering anisotropy to changes in the micelle and network structure, the alignment factor (A_f) was calculated from the scattering data using Equation 1. The alignment factor as a function of shear rate is presented in Figure 7.

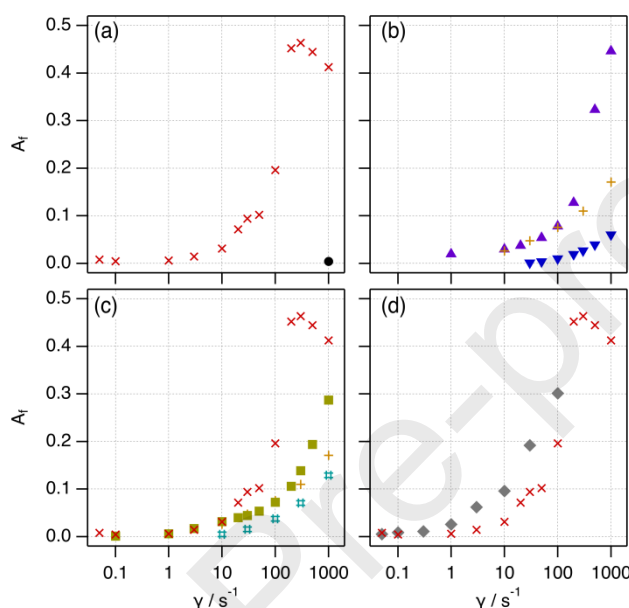


Figure 7. Alignment factor versus shear rate for the C_{16}G_2 system in D_2O at different conditions: (a) 100 mM $\alpha\text{-C}_{16}\text{G}_2$ (●) and $\beta\text{-C}_{16}\text{G}_2$ (×) at $50\text{ }^\circ\text{C}$; (b) different mixing ratios: 75% β /25% α (▲), 50% β /50% α (+), and 25% β /75% α (▼); (c) 100 mM 100% $\beta\text{-C}_{16}\text{G}_2$ at $50\text{ }^\circ\text{C}$ (×) and $30\text{ }^\circ\text{C}$ (■) and 50% β /50% α at $50\text{ }^\circ\text{C}$ (+) and $30\text{ }^\circ\text{C}$ (#); and (d) $\beta\text{-C}_{16}\text{G}_2$ at $50\text{ }^\circ\text{C}$ at 200 (◆) and 100 mM (×).

As foreseen for the change in 2D scattered intensity, the anisotropy in the scattering data must arise from some structural rearrangement induced by the stress applied. One of the common mechanisms associated with the shear-thinning behaviour of WLM is the alignment of micelles under stress [8]. The alignment factor is a parameter used to quantify the degree of directional alignment of the micelles when shear is applied to the sample. For all samples containing $\beta\text{-C}_{16}\text{G}_2$, A_f increases with increasing shear rate and plateaus at *ca.* 0.45 above 200 s^{-1} . This is probably the shear rate at which the micelles reach equal alignment over the Couette gap. This has previously been showed for mixtures of CTAT and SDBS in D_2O [16]. The lower boundary case is obtained for 100 mM $\alpha\text{-C}_{16}\text{G}_2$ (0% $\beta\text{-C}_{16}\text{G}_2$), as this sample only displays minor alignment at the highest shear rate (1000 s^{-1}), as previously seen for the angle-dependant scattering. This distinct behaviour is attributed to the significantly shorter micelles of $\alpha\text{-C}_{16}\text{G}_2$ in comparison to the WLM formed by $\beta\text{-C}_{16}\text{G}_2$ based on the investigations using static SANS [23].

For the surfactant mixtures, the A_f at a given shear rate monotonically decreases with decreasing ratio of $\beta\text{-C}_{16}\text{G}_2$, but even at the lowest β -content (i.e. 25% $\beta\text{-C}_{16}\text{G}_2$) shows a certain degree of alignment: A_f is about the same for 50, 75 and 100% $\beta\text{-C}_{16}\text{G}_2$ in the surfactant anomer mixture at a shear rate of 10 s^{-1} ; at higher shear rates, the alignment for 50 and 75% $\beta\text{-C}_{16}\text{G}_2$ is similar, while it is higher for 100% $\beta\text{-C}_{16}\text{G}_2$; and the A_f -values for 25% $\beta\text{-C}_{16}\text{G}_2$ are lower than those for higher $\beta\text{-C}_{16}\text{G}_2$ ratios in the entire shear rate range. Therefore, the boundary values are shown by the scattering from the two pure anomers, where the highest A_f is observed for 100% $\beta\text{-C}_{16}\text{G}_2$, the smallest A_f appears for 100% $\alpha\text{-C}_{16}\text{G}_2$, and the values for the surfactant mixtures fall in between those two.

Discussion

The interesting rheological behaviour of hexadecylmaltosides with different anomeric configuration has been previously hypothesised to relate to the structure of the micelles [22, 23]. The differences in micelle structure have been attributed to how the monomers interact in the micelle depending on the anomeric configuration of the surfactant, despite being identical in terms of chemical composition. As such, the formation of an extensive hydrogen bond network between neighbouring headgroups was reported for the β -configuration of dodecylmaltoside [35], which is hypothesised to differ from that between α -anomers. Therefore, this difference in the molecular interactions is expected to drive the formation of micelles with different morphologies and scission energies [23, 35, 36].

From the results presented here, the shear-thinning behaviour of the elongated micelles is attributed to the segmental alignment of micelles in the direction of the flow. This has been shown to be the mechanism for several WLM systems [9, 15, 21, 37]. When comparing the rheological properties of the samples (See Figure 2) with the A_f values (See Figure 7), some observations can be made. Although high shear rates clearly induce micellar alignment, changes in the viscosity of the system already appear at lower shear rates. For example, for 100 mM β -C₁₆G₂ shear thinning starts at shear rates of *ca.* 0.1 s⁻¹ whilst A_f starts to increase around 1 s⁻¹, and at 1 s⁻¹ the viscosity has decreased by one order of magnitude. This disconnect between the microscopic structure and the rheology could be attributed to structural rearrangements induced by shear in a larger length scale than that which is accessible in the experimental setup used here, while maintaining isotropy in a segmental scale [19].

For the systems showing the same viscosity values at a certain point in the flow curve (100, 75 and 50% β -C₁₆G₂), the variations in A_f with shear rate follow the same trend but the absolute values are shifted (see Figure 7a and b). Considering the previous investigations using oscillatory rheology, an increase in the β -C₁₆G₂ ratio prompts a behaviour that is close to that of a Maxwellian fluid [23]. For a Maxwellian fluid, micelle scission becomes the dominant relaxation mode and, thus, micelles break faster than they reptate along their contour length when stress is applied [6]. One possible explanation for the differences in the A_f values, despite the samples showing the same viscosity values, is that the relaxation mode of the system is intrinsically connected to the length of the micelle and intermicellar interaction. Although higher β -C₁₆G₂ contents result in longer micelles, micelle breakage becomes the dominant relaxation mode. Thus, the longer micelles are more likely to break into small segments, which easily align under flow and the viscosity decreases. However, the case for micelles with lower β -C₁₆G₂ ratios is different. These systems were shown to deviate from the Maxwellian behaviour and, thus, micelle breakage is less dominant. This potentially results in longer segments for which the rotational diffusion is slower, prompts a less pronounced segmental alignment and similar viscosity values at certain shear rates (i.e. between 10 and 100 s⁻¹). Therefore, global effects (entanglement and breaking) and local effects (volume exclusion and alignment of neighbouring sections) coexist at different length scales.

Changes in temperature have also been shown to have an effect in the rheology of the system. This was again related to the morphology of the micelles, as micelles were seen to increase in length from 30 °C to 50 °C for both 100% β -C₁₆G₂ and 50% β -C₁₆G₂ in the dilute regime [23]. These differences are also reflected in the structure of the system under shear, as A_f is lower at 30 °C compared to 50 °C (see Figure 7c). Also, 100% β -C₁₆G₂ shows higher A_f -values than 50% β -C₁₆G₂ at each temperature. This again relates to the structure of the micelles and intermicellar interactions in the system. As micelles are longer at 50 °C the viscosity is higher and the slower rotational diffusion results in a more pronounced alignment, whilst the interactions between micelles are similar at both temperatures [23]. This could be attributed to the temperature-induced dehydration of the headgroup region of the micelles [22], which would strengthen the interactions and disfavour scission.

A comparison of the alignment of β -C₁₆G₂ at two different concentrations (100 and 200 mM) reveals that the onset of alignment starts at lower shear rate for the higher concentration, as seen in Figure 7d. The shear rate dependence is similar for the two concentrations between 1 and 100 s⁻¹. The difference in the A_f -values can therefore be related to an increase in the intermicellar interactions, as an increase in concentration was seen to have a minor effect in the elongation of the micelles. As the volume fraction of micelles increases, the entanglement of the network also increases and with more entanglement the alignment upon shear becomes more pronounced. It shall be noted that for the 200 mM samples, above 100 s⁻¹ the anisotropy is lost, and the scattered intensity drastically decreases. This is believed to be caused by the high shear which causes highly turbulent flow for that sample. This effect introduces bubbles which

decreased the effective scattering volume inside the Couette. However, it is hypothesised that the alignment of micelles would also plateau at A_f *ca.* 0.45.

The increase in the scattering signal at low q at high shear rates (See Figure 5) must relate to the formation of correlations at larger length scales induced by the shear. As this signal dominates in the vertical projection of the scattering, the density correlations are expected to show anisotropy. This characteristic signal has previously been attributed to the shear-induced formation of anisotropic domains which orient along the direction of the flow. These large domains are mostly populated by branched networks for other micellar systems [38]. Also, no evidence was found for shear banding in these systems, as has been shown for other WLM systems. Calabrese et. al. reported how shear banding is displayed in the 2D detector images for the 1-3 scattering plane, with a combination of isotropic and anisotropic scattering [16]. These features were not found in the scattering data presented here. Another sign of the absence of shear banding for the systems investigated here is a continuous flow curve without hysteresis, as previously reported [19]. An exception to this is seen at the highest investigated concentration (200 mM β -C₁₆G₂), where a discontinuity in the flow curve is observed at low shears. At this concentration a thixotropic behaviour was observed, which could indicate changes in the formation of macroscopic concentration fluctuations. However, no direct evidence has been obtained with the characterisation performed here. A possible explanation for the absence of shear banding at the lower β -C₁₆G₂ concentrations is that the presence of branches in the micelles, instead of entanglement points, hinders shear banding [19]. This could be also evidenced by the low A_6 , as no higher values than 0.45 are reached, and branching lowers the A_f values. Further investigations are required to determine the structure of the large flow-induced domains in the present systems and the role of other flow heterogeneities in the behaviour of the system.

Conclusions

The self-assembly of hexadecylmaltoside has been shown to result in a fluid that acts as a rheological modifier, inducing shear-thinning behaviour with tailorable viscosity. Here, we have investigated the origin of this behaviour, relatively unexplored for non-ionic surfactants [3, 20, 21]. As shown by the morphological characterisation of the micelles in the semi-dilute regime under no shear, α -C₁₆G₂ forms weakly interacting elongated micelles with contour lengths around 1400 Å and β -C₁₆G₂ forms strongly correlated WLM with contour lengths around 10,000 Å. Thus, the structural features of the micelles in the dilute regime persist even at higher concentrations [22, 23]. Considering the rheological behaviour and previous investigations of the micellar morphology of the mixed micelles, it is hypothesised that the micelle morphology in the dilute regime can also be extrapolated to the semi-dilute regime for those, thus forming micelles with intermediate morphologies to those of the pure anomers.

Upon shear, the entangled network of WLM formed by β -C₁₆G₂ begins to align, whilst the shorter rod-like aggregates of α -C₁₆G₂ only show weak alignment at very high shear rates. This is connected to the rheology of each system, as the longer micelles result in shear-thinning behaviour and the shorter aggregates show minor changes in the rheological behaviour of the system. Thus, segmental alignment in the direction of the flow correlates with the reduction of viscosity for the WLM systems. This interpretation is also extended to the surfactant mixtures, as higher ratios of β -C₁₆G₂ lead to more viscous systems in connection to the formation of longer micelles. A decrease in alignment is observed for decreasing ratio of β -C₁₆G₂, which connects to the formation of shorter micelles as seen in the dilute regime [23].

Variations in concentration and temperature also showed an effect in the resulting rheology that is connected to the structure of the micelles and intermicellar interactions. At the higher β -C₁₆G₂ concentration, 200 mM, the alignment is more pronounced in comparison to the lower concentrated sample, 100 mM. This was attributed to the formation of a more entangled network at higher surfactant concentration which was more prone to align upon shear. Interestingly, temperature induces a similar change in the behaviour of the system. It has been previously shown that an increase in temperature counterintuitively leads to an increase in the viscosity of the system [23]. As the volume fraction of micelles is rather similar at the two temperatures investigated here, the differences in the rheological behaviour and alignment must be attributed to differences in micelle morphology. As such, higher temperatures, which have been shown to induce the formation of longer micelles, result in a more entangled micellar network. This leads to earlier and more pronounced alignment upon shear, as observed in the rheo-SANS results.

Previous rheological characterisation of the system showed that, with increasing micelle volume fraction or length, micelle breakage became the dominant relaxation mode upon shear [23]. Based on this rheo-SANS results, the observed alignment arises from the orientation of micelle segments in the direction of the flow. As such, the mechanism of the rheological modification induced by the self-assembly of α - and β -C₁₆G₂ is shown to be connected to the nanoscale structure of the micelles. These results provide a detailed understanding on the function-structure relationship of the sugar-based self-assemblies, assisting the development of new technologies, such as response materials and drag-reducing agents, based on these sustainable surfactants [1]. Also, this knowledge will guide the design and synthesis of new sugar-based surfactants with tailorable molecular structure, self-assembly, and function [39]. In addition, a rework of the previously published PRISM model is presented, expanding the applicability of the model to a wider variety of anisotropic micelles [28].

Acknowledgements

The Authors would like to thank the Swedish Research Council Formas (Grant 2015-666) for funding J.L. The research was also performed with financial support from Vinnova - Swedish Governmental Agency for Innovation Systems within the NextBioForm Competence Centre. This work is based upon experiments performed on the D22 instrument at Institut Laue-Langevin (Proposal No. 9-10-1610).

CRediT authorship contribution statement

Johan Larsson: Methodology, Investigation, Formal analysis, Writing - original draft. **Ashley P. Williams:** Investigation, Software, Formal analysis, Writing - review & editing. **Marie Wahlgren:** Methodology, Writing - review & editing. **Lionel Porcar:** Investigation, Resources, Writing - review & editing. **Stefan Ulvenlund:** Methodology, Writing - review & editing, Funding acquisition. **Tommy Nylander:** Methodology, Writing - review & editing, Funding acquisition. **Rico F. Tabor:** Methodology, Software, Writing - review & editing. **Adrian Sanchez-Fernandez:** Conceptualization, Methodology, Formal analysis, Writing - review & editing.

Declaration of Competing Interest

The authors declare that they have no known competing financial interests or personal relationships that could have appeared to influence the work reported in this paper.

References

- [1] W. von Rybinski, K. Hill, Alkyl Polyglycosides—Properties and Applications of a new Class of Surfactants, *Angew. Chem. Int. Ed.* 37(10) (1998) 1328-1345.
- [2] J. Yang, Viscoelastic wormlike micelles and their applications, *Current Opinion in Colloid & Interface Science* 7(5) (2002) 276-281.
- [3] C.A. Dreiss, Wormlike micelles: where do we stand? Recent developments, linear rheology and scattering techniques, *Soft Matter* 3(8) (2007) 956-970.
- [4] S. Ezrahi, E. Tuval, A. Aserin, Properties, main applications and perspectives of worm micelles, *Adv. Colloid Interface Sci.* 128-130 (2006) 77-102.
- [5] Z. Chu, C.A. Dreiss, Y. Feng, Smart wormlike micelles, *Chem. Soc. Rev.* 42(17) (2013) 7174-7203.
- [6] M. Cates, Reptation of living polymers: dynamics of entangled polymers in the presence of reversible chain-scission reactions, *Macromolecules* 20(9) (1987) 2289-2296.
- [7] B.F. García, S. Saraji, A new insight into the dependence of relaxation time on frequency in viscoelastic surfactant solutions: From experimental to modeling study, *J. Colloid Interface Sci.* 517 (2018) 265-277.
- [8] B. Arenas-Gómez, C. Garza, Y. Liu, R. Castillo, Alignment of worm-like micelles at intermediate and high shear rates, *J. Colloid Interface Sci.* 560 (2020) 618-625.
- [9] M. Takeda, T. Kusano, T. Matsunaga, H. Endo, M. Shibayama, T. Shikata, Rheo-SANS Studies on Shear-Thickening/Thinning in Aqueous Rodlike Micellar Solutions, *Langmuir* 27(5) (2011) 1731-1738.
- [10] J.E. López-Aguilar, M.F. Webster, H.R. Tamaddon-Jahromi, O. Manero, A new constitutive model for worm-like micellar systems – Numerical simulation of confined contraction–expansion flows, *Journal of Non-Newtonian Fluid Mechanics* 204 (2014) 7-21.
- [11] A.P.R. Eberle, L. Porcar, Flow-SANS and Rheo-SANS applied to soft matter, *Current Opinion in Colloid & Interface Science* 17(1) (2012) 33-43.
- [12] M.A. Calabrese, N.J. Wagner, Chapter 8. New Insights from Rheo-small-angle Neutron Scattering, Wormlike Micelles, *The Royal Society of Chemistry* 2017, pp. 193-235.

- [13] J.B. Hayter, J. Penfold, Use of viscous shear alignment to study anisotropic micellar structure by small-angle neutron scattering, *J. Phys. Chem.* 88(20) (2002) 4589-4593.
- [14] V.T. Kelleppan, J.E. Moore, T.M. McCoy, A.V. Sokolova, L.d. Campo, B.L. Wilkinson, R.F. Tabor, Self-Assembly of Long-Chain Betaine Surfactants: Effect of Tailgroup Structure on Wormlike Micelle Formation, *Langmuir* 34(3) (2018) 970-977.
- [15] S. Förster, M. Konrad, P. Lindner, Shear Thinning and Orientational Ordering of Wormlike Micelles, *Phys. Rev. Lett.* 94(1) (2005) 017803.
- [16] M.A. Calabrese, S.A. Rogers, L. Porcar, N.J. Wagner, Understanding steady and dynamic shear banding in a model wormlike micellar solution, *J. Rheol.* 60(5) (2016) 1001-1017.
- [17] M.E. Helgeson, P.A. Vasquez, E.W. Kaler, N.J. Wagner, Rheology and spatially resolved structure of cetyltrimethylammonium bromide wormlike micelles through the shear banding transition, *J. Rheol.* 53(3) (2009) 727-756.
- [18] T. Divoux, M.A. Fardin, S. Manneville, S. Lerouge, Shear Banding of Complex Fluids, *Annual Review of Fluid Mechanics* 48(1) (2016) 81-103.
- [19] M.W. Liberatore, F. Nettesheim, P.A. Vasquez, M.E. Helgeson, N.J. Wagner, E.W. Kaler, L.P. Cook, L. Porcar, Y.T. Hu, Microstructure and shear rheology of entangled wormlike micelles in solution, *J. Rheol.* 53(2) (2009) 441-458.
- [20] P.G. Cummins, E. Staples, J. Penfold, R.K. Heenan, The geometry of micelles of the poly(oxyethylene) nonionic surfactants C16E6 and C16E8 in the presence of electrolyte, *Langmuir* 5(5) (1989) 1195-1199.
- [21] J.E. Moore, T.M. McCoy, L. de Campo, A.V. Sokolova, C.J. Garvey, G. Pearson, B.L. Wilkinson, R.F. Tabor, Wormlike micelle formation of novel alkyl-tri(ethylene glycol)-glucoside carbohydrate surfactants: Structure–function relationships and rheology, *J. Colloid Interface Sci.* 529 (2018) 464-475.
- [22] J. Larsson, A. Sanchez-Fernandez, N. Mahmoudi, L.C. Barnsley, M. Wahlgren, T. Nylander, S. Ulvenlund, Effect of the Anomeric Configuration on the Micellization of Hexadecylmaltoside Surfactants, *Langmuir* 35(43) (2019) 13904-13914.
- [23] J. Larsson, A. Sanchez-Fernandez, A.E. Leung, R. Schweins, B. Wu, T. Nylander, S. Ulvenlund, M. Wahlgren, Molecular structure of maltoside surfactants controls micelle formation and rheological behavior, *J. Colloid Interface Sci.* 581(Pt B) (2021) 895-904.
- [24] Grasp, 2020. <https://www.ill.eu/users/support-labs-infrastructure/software-scientific-tools/grasp/>. (Accessed 2020-12-07).
- [25] L. Cannavacciuolo, J.S. Pedersen, P. Schurtenberger, Monte Carlo Simulation Study of Concentration Effects and Scattering Functions for Polyelectrolyte Wormlike Micelles, *Langmuir* 18(7) (2002) 2922-2932.
- [26] J.S. Pedersen, P. Schurtenberger, Scattering Functions of Semiflexible Polymers with and without Excluded Volume Effects, *Macromolecules* 29(23) (1996) 7602-7612.
- [27] W.R. Chen, P.D. Butler, L.J. Magid, Incorporating intermicellar interactions in the fitting of SANS data from cationic wormlike micelles, *Langmuir* 22(15) (2006) 6539-48.
- [28] A.P. Williams, J.P. King, A.V. Sokolova, L. de Campo, R.F. Tabor, In Situ Nanostructural Analysis of Concentrated Wormlike Micellar Fluids Comprising Sodium Laureth Sulfate and Cocamidopropyl Betaine Using Small-Angle Neutron Scattering, *Langmuir* 36(47) (2020) 14296-14305.
- [29] M. Kotlarchyk, R.B. Stephens, J.S. Huang, Study of Schultz distribution to model polydispersity of microemulsion droplets, *J. Phys. Chem.* 92(6) (1988) 1533-1538.
- [30] J. Larsson, L. Porcar, M. Wahlgren, T. Nylander, S. Ulvenlund, A. Sanchez-Fernandez, Structural effects of flow on elongated alkylglycoside micelles, *Insitut Laue-Langevin (ILL)*, 2020, 10.5291/ILL-DATA.9-10-1610.
- [31] C.A. Ericsson, O. Söderman, V.M. Garamus, M. Bergström, S. Ulvenlund, Effects of Temperature, Salt, and Deuterium Oxide on the Self-Aggregation of Alkylglycosides in Dilute Solution. 1. n-Nonyl- β -D-glucoside, *Langmuir* 20(4) (2004) 1401-1408.
- [32] C.A. Ericsson, O. Soderman, V.M. Garamus, M. Bergstrom, S. Ulvenlund, Effects of temperature, salt, and deuterium oxide on the self-aggregation of alkylglycosides in dilute solution. 2. n-Tetradecyl-beta-D-maltoside, *Langmuir* 21(4) (2005) 1507-15.
- [33] G.T. Keep, R. Pecora, Reevaluation of the dynamic model for rotational diffusion of thin, rigid rods in semidilute solution, *Macromolecules* 18(6) (2002) 1167-1173.
- [34] J.-F. Berret, R. Gamez-Corrales, J. Oberdisse, L. Walker, P. Lindner, Flow-structure relationship of shear-thickening surfactant solutions, *EPL (Europhysics Letters)* 41(6) (1998) 677.
- [35] M. Kanduc, E. Schneck, C. Stubenrauch, Intersurfactant H-bonds between head groups of n-dodecyl-beta-d-maltoside at the air-water interface, *J. Colloid Interface Sci.* 586 (2021) 588-595.
- [36] G. Zaldivar, M. Conda-Sheridan, M. Tagliazucchi, Scission energies of surfactant wormlike micelles loaded with nonpolar additives, *J. Colloid Interface Sci.* (2021).
- [37] J.E. Moore, T.M. McCoy, A.V. Sokolova, L. de Campo, G.R. Pearson, B.L. Wilkinson, R.F. Tabor, Worm-like micelles and vesicles formed by alkyl-oligo(ethylene glycol)-glycoside carbohydrate surfactants: The effect of precisely tuned amphiphilicity on aggregate packing, *J. Colloid Interface Sci.* 547 (2019) 275-290.
- [38] B.A. Schubert, N.J. Wagner, E.W. Kaler, S.R. Raghavan, Shear-Induced Phase Separation in Solutions of Wormlike Micelles, *Langmuir* 20(9) (2004) 3564-3573.
- [39] J. Larsson, A.E. Leung, C. Lang, B. Wu, M. Wahlgren, T. Nylander, S. Ulvenlund, A. Sanchez-Fernandez, Tail unsaturation tailors the thermodynamics and rheology of a self-assembled sugar-based surfactant, *J. Colloid Interface Sci.* 585 (2021) 178-183.

Declaration of interests

☒ The authors declare that they have no known competing financial interests or personal relationships that could have appeared to influence the work reported in this paper.

☐ The authors declare the following financial interests/personal relationships which may be considered as potential competing interests:

